UNIVERSITY OF WATERLOO
Faculty of Science

Analysis of recent two- and three-body nuclear interactions

Theory Group - TRIUMF
Vancouver, British Columbia

prepared by

Michael Gennari
#20552297
4A Mathematical Physics
December 2017

1330 Burrard Street
Vancouver, BC
V6Z 2B7

January 5, 2018

Brian McNamara
Physics and Astronomy
University of Waterloo
Waterloo, Ontario
V6T 2A3

Dear Brian McNamara,

I have prepared the enclosed report *"Analysis of recent two- and three-body nuclear interactions"* as my 4A Work Report for TRIUMF. This report, the third of four work reports that Co-operative Education Program requires that I complete as part of my Co-op BSc degree requirements, has not received previous academic credit.

The Theory Group at TRIUMF, led by my supervisor Petr Navrátil, focuses on *ab initio* approaches to theories in nuclear and particle physics. As a researcher in theoretical nuclear physics at TRIUMF, I assisted Dr. Petr Navrátil in performing extensive analysis of high precision two- and three-nucleon interactions, which are the only input for our *ab initio* calculations. It should be noted that this project represents a fraction of the entire term, the rest of which was spent completing a previous project on nonlocal nuclear densities, writing a publishable work for that project, and beginning a new project on natural basis representations in nuclear physics.

This report was written entirely by myself and has not received previous academic credit at any institution. I would like to thank Dr. Petr Navrátil, Dr. Matteo Vorabbi, and Dr. Angelo Calci for assisting and guiding me with my work throughout the past several terms at TRIUMF. I give permission to TRIUMF to keep this report on file and use it for internal reporting and external reporting including publication.

Sincerely,

Michael Gennari

Encl.

ABSTRACT: Analysis of recent two- and three-body nuclear interactions

The construction of two- and three-nucleon chiral effective field theory (EFT) potentials provide a systematic way to incorporate complex many-body nuclear dynamics in computations of various nuclear observables using frameworks such as the no-core shell model (NCSM). In the past, primarily two-body interactions have been used to make theoretical predictions in nuclear physics given the complexity of higher-body terms. In this work, we discuss the recent inclusion of high quality three-body interactions and we analyze the effects of incorporating these three-body potentials into our calculations, using the two-body results as a benchmark. We find that two- plus three-body potentials significantly improve our ability to make accurate predictions using an *ab initio* framework. The results for the ground state energy and excitation spectra of ^{4,6}He, ^{6,7,8}Li, ^{10}B, ^{12}C, and ^{16}O are shown to illustrate the significance of including three-body terms, and potentially higher-body terms, in our calculations.

Contents

List of Figures

1.0 Introduction

In this work we will be analyzing two- and three-body terms in the no-core shell model (NCSM) constructed from chiral effective field theory for nuclear interactions [1]. Data has been analyzed to produce plots for the ground state energy convergence of nuclei, the spectra of excited states of nuclei, and overlaps of the wave functions of nuclei. Only ground state convergence and excitation spectra will be discussed in section 2.0 .

The NCSM framework is the model we employ in our calculations of nuclear observables [2]. In this model, nuclei are treated as A nucleon systems of point-like, non-relativistic nucleons interacting via inter-nucleon potentials, of which the most dominant contributions appear to be two- and three-body interactions. All A nucleons are considered active degrees of freedom and, in this model, the translational invariance of observables, angular momentum, and parity for the nucleus are conserved. The wave functions constructed in the NCSM basis are computed by diagonalizing the translationally invariant nuclear Hamiltonian,

$$\hat{H} \left| A\lambda J^{\pi} T \right\rangle = E_{\lambda}^{J^{\pi}T} \left| A\lambda J^{\pi} T \right\rangle \ , \tag{1}$$

which includes two-nucleon (NN) forces, and more generally, will also include three-nucleon interactions ($3N$). λ characterizes additional quantum numbers of eigenstates with identical $J^{\pi}T$. The many-body wave function constructed from the NCSM eigenstates is expanded over a complete set of antisymmetric A-nucleon harmonic oscillator (HO) basis states. Given that we expand the NCSM states in terms of the harmonic oscillator basis, we have an $\hbar\Omega$ parameter which characterizes the frequency and center of the

HO well. The truncation of the basis states is handled by including basis states above the lowest configuration of the nucleons up to a maximum of $N_{\max}$ HO excitations, $N_0 \leq N = 2n + l \leq N_{\max}$. Thus, by increasing the $N_{\max}$ parameter, we incorporate higher level excitations of the nucleus in question and approach the converged result. While reasonable results can be calculated for very light nuclei ($A \leq 4$) using the bare interaction, we require faster convergence of the HO expansion in order to obtain reasonable results for higher $A-$nucleon systems. By introducing similarity renormalization groups (SRG), which introduce flow equations into the nuclear Hamiltonian problem as according to Ref. [3, 4, 5, 6], we can accelerate convergence of larger $N_{\max}$ calculations by evolving the NN and $3N$ interactions. This technique guarantees faster convergence. However, if the unitarity of the transformation is violated by truncations, it introduces an additional parameter dependence on the momentum-decoupling scale labeled as λ_{SRG}. If convergence is achieved, the dependence on λ_{SRG} should vanish. When possible, we show results for the bare, unevolved interactions and compare with the transformed interactions in order to show that there is consistency in the results produced. The extrapolation result provided in each figure, $E_{ext.}$, is shown with the lowest possible λ_{SRG} parameter.

The results of this work have been computed using a two-body (NN) chiral potential at fifth order [7] with an energy cut-off of $\Lambda = 500$ MeV included in the regulator function to deal with infinities in the Lippmann-Schwinger (LS) equation, detailed in Ref. [8, 9, 10, 11]. In addition, we show results including three-body potentials (3N) at next-to-next-to leading order (N^2LO) with simultaneous local and nonlocal regularization [12, 21]. Cut-offs for the local part of the interaction are made at 650 MeV and nonlocal cut-offs are made at 500 MeV.

Even with work to improve convergence of results, when we move our calculations to larger $A-$nucleon systems, we continue to encounter issues due to the rapid basis size expansion. Thus, it is important for us to introduce additional truncations which will induce only minor errors in our wave functions. One such truncation method involves introducing a parameter, κ_{min}, which reduces the basis size according to the size of wave functions corrections for given eigenstates. This way, we can directly control the accuracy of these larger calculations and ensure they converge to a result within reasonable computation times. When employing this truncation method and analyzing ground state convergence results, it is possible to extrapolate results for several different values of κ_{min} with a quadratic fit in order to produce expected results for $\kappa_{min} = 0$. Once this is done, we can employ exponential extrapolation of the form,

$$f(N_{max}) = E_\infty + Ae^{-bN_{max}} \ , \tag{2}$$

using the three largest $N_{\max}$ calculations. This allows us to exactly determine the coefficients E_∞, A, and b and thus obtain the $N_{\max} \to \infty$ result for our ground state energy. Results for the spectra of nuclei simply use the lowest possible κ_{min} values.

All experimental results shown for ground state energies and nuclear excitation spectra are taken from the Triangular Universities Nuclear Laboratory (TUNL) Nuclear Data Evaluation Group [13, 14, 15, 16, 17]. Note that states which have no corresponding experimental value are currently considered unphysical predictions by the NCSM.

2.0 Two- and three-body interaction analysis

2.1 Two-body interactions

2.1.1 Ground state energy convergence

The two-body potentials for which results are presented have been computed to fifth order of a chiral effective field theory (EFT) expansion for the two-nucleon (NN) interaction, as described in Ref. [7]. These nonlocal potentials are considered high quality and consistent due to their use of identical power counting schemes and energy cut-off procedures applied to all orders, with long-range components of the interactions being fixed by highly accurate constraints for the low energy coefficients. The maximum order achieved is fifth order, labeled as next-to-next-to-next-to-next-to-leading order (N^4LO). This NN component of the potentials serves as a strong basis for our *ab initio* nuclear structure calculations. Further, we shall denote this contribution to the nuclear potential as $NN - N^4LO(500)$, where NN refers to the two-body component, N^4LO refers to the chiral EFT truncation, and 500 refers to the energy cut-off of 500 MeV.

All results shown use the fastest converging SRG value available, with decreasing λ_{SRG} improving convergence. When possible, the bare, unevolved interaction is used in order to show that when convergence is achieved with either type, the results achieved are consistent with one another.

In Fig. 1, we show results for the convergence of the ground state energies of ^{4}He using the $NN - N^4LO(500)$ interaction. As expected, the smaller the

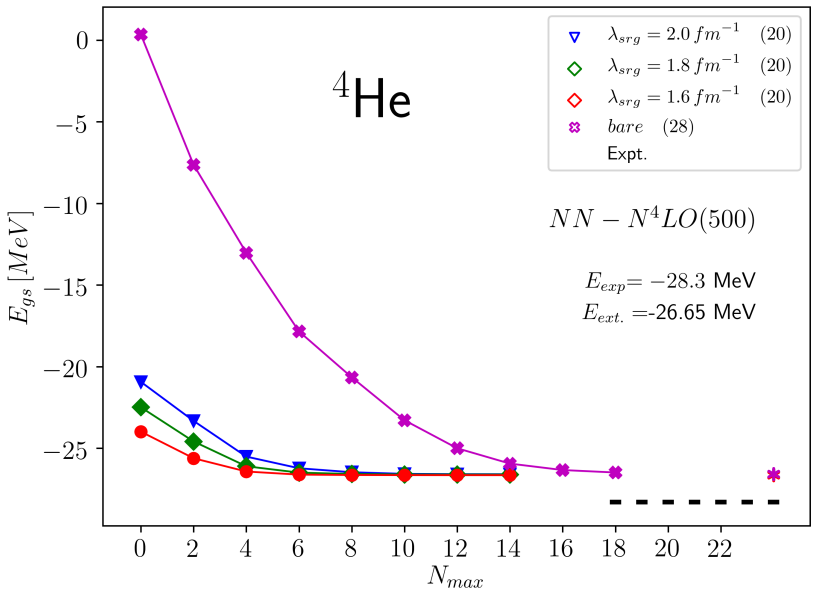

Figure 1: Convergence of ground state energy for ^{4}He using the $NN - N^4LO(500)$ interaction. SRG parameters of 2.0, 1.8, and 1.6 fm^{-1} are shown using an $\hbar\Omega = 20$ MeV, along with the bare interaction shown using $\hbar\Omega = 28$ MeV. Extrapolated energies are shown with starred markers. Experimental data is shown with black lines.

SRG wave flow parameter the faster we are able to achieve convergence with the interactions. There is a significant difference between the convergence rates of SRG evolved and the bare interactions, as can be seen in the figure. However, once convergence is reached, we do achieve the same result as is expected. It is clear that SRG evolution improves convergence rates significantly, making it a necessary procedure to apply in larger $A-$nucleon systems as the bare interaction does not converge rapidly enough. Notably, we see that the extrapolated values are different from experimental values by nearly 2 MeV. This means the nuclear potential is under-binding the nucleus and we are producing radii larger than we should. Similar results can be seen in Fig. 2 and 3, where the under-binding is more significant. Extrapolated values differ from experimental results by about 5 MeV for ^{6}He and about 2 MeV for ^{6}Li.

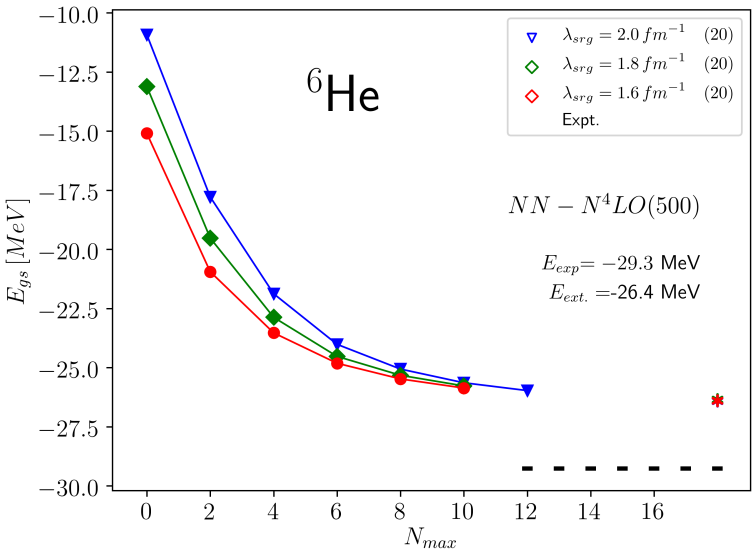

Figure 2: Convergence of ground state energy for ^{6}He using the $NN - N^4LO(500)$ interaction. SRG parameters of 2.0, 1.8, and 1.6 fm^{-1} are shown using an $\hbar\Omega = 20$ MeV. Extrapolated energies are shown with starred markers. Experimental data is shown with black lines.

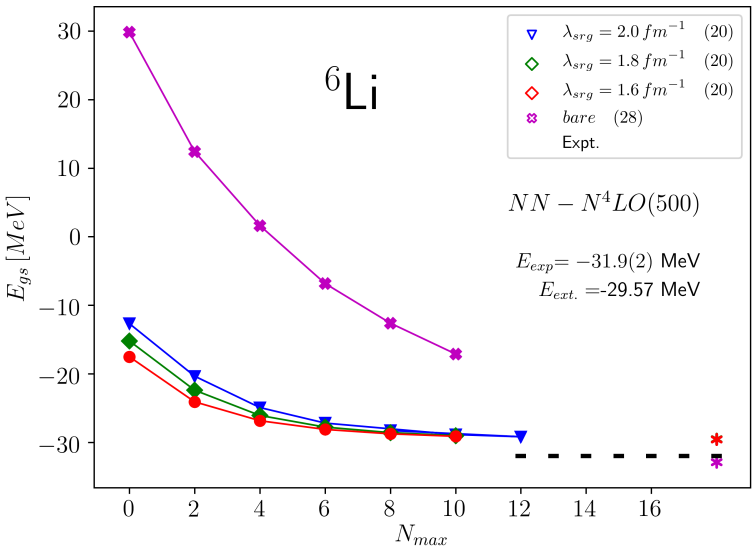

Figure 3: Convergence of ground state energy for ^{6}Li using the $NN - N^4LO(500)$ interaction. SRG parameters of 2.0, 1.8, and 1.6 fm^{-1} are shown using an $\hbar\Omega = 20$ MeV, along with a bare interaction at $\hbar\Omega = 28$ MeV. Extrapolated energies are shown with starred markers. Experimental data is shown with black lines.

Such large differences in ^{6}He are not surprising given the halo structure of the nucleus. The central alpha core being orbited by a two-neutron pair makes for complicated nuclear dynamics by combining effects from both short-range and long-range contributions in the potentials. This is, in general, a difficult problem in nuclear theory to solve. Notice, in Fig. 3, that the extrapolated value of the bare interaction tends to fall below the SRG evolved extrapolated points. This is incorrect given that the SRG evolved interactions are constructed in a way which preserves the properties of the bare interaction. Thus, our method of extrapolation cannot be applied to the ^{6}Li bare interaction as the results have not converged rapidly enough to yield good extrapolated results. Similar discrepancies can be seen in SRG evolved interactions of larger $A-$body systems such as ^{12}C and ^{16}O, shown in Fig. 4 and Fig. 5, respectively.

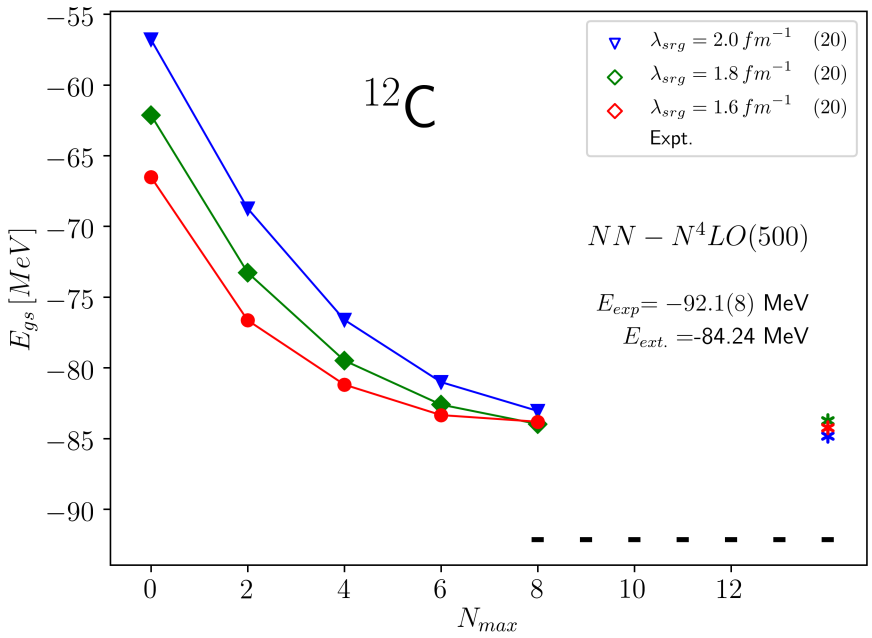

Figure 4: Convergence of ground state energy for ^{12}C using the $NN - N^4LO(500)$ interaction. SRG parameters of 2.0, 1.8, and 1.6 fm^{-1} are shown using an $\hbar\Omega = 20$ MeV. Extrapolated energies are shown with starred markers. Experimental data is shown with black lines.

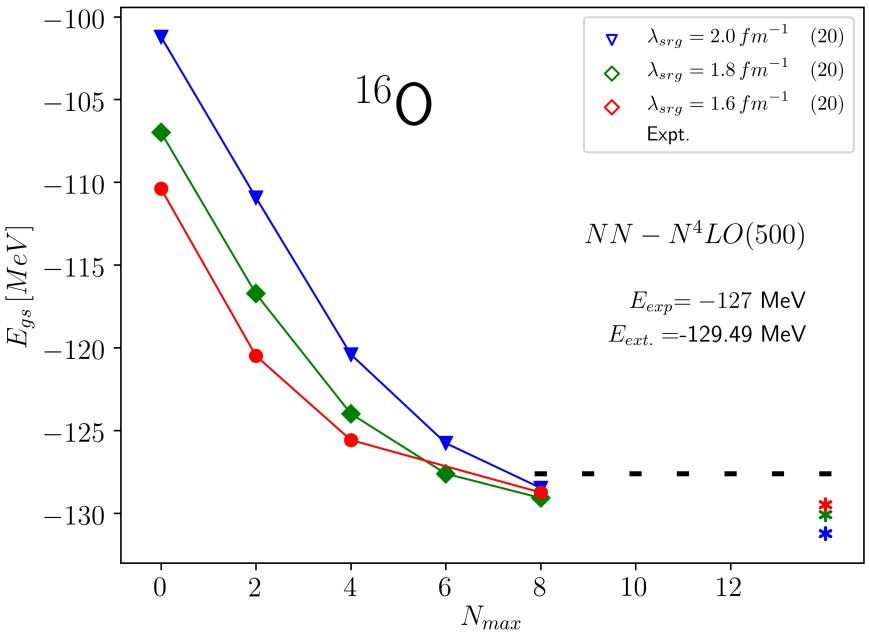

Figure 5: Convergence of ground state energy for ^{16}O using the $NN - N^4LO(500)$ interaction. SRG parameters of 2.0, 1.8, and 1.6 fm^{-1} are shown using an $\hbar\Omega = 20$ MeV. Extrapolated energies are shown with starred markers. Experimental data is shown with black lines.

The situation is more serious here as we observe higher dependencies on the SRG parameter, to the point where some cross. It is ideal, then, that we perform additional calculations with larger runtimes in order to produce converged results for the necessary $N_{\max}$ values of the larger systems.

We have seen that the $NN - N^4LO(500)$ interaction under binds the nucleus, even in the case of smaller nuclei. This motivates the inclusion of additional higher body interactions such as a 3N interaction, in order to provide more reasonable agreement with results. With this, we must ensure not to hinder convergence speeds of the interactions as that will results in complications with higher $N_{\max}$ calculations.

2.1.2 Excitation spectra

We will now study the excitation spectra of different nuclei using the $NN - N^4LO(500)$ potential. Using the NCSM, it is possible to calculate information about various nuclear states, as well as transitions between states during processes such as beta decays.

In Fig. 6, we have results of the excitation spectra of ^{10}B. This is an interesting nucleus to study using the NCSM since we see a change in what occupies the ground state. This plot is adjusted to push the $(3^+, 0)$ state below a relative energy of 0 MeV in order to maintain a consistent ground state. Notice though, that with increasing $N_{\max}$ we find that the $(3^+, 0)$ moves from the first possible state to the first excited state.

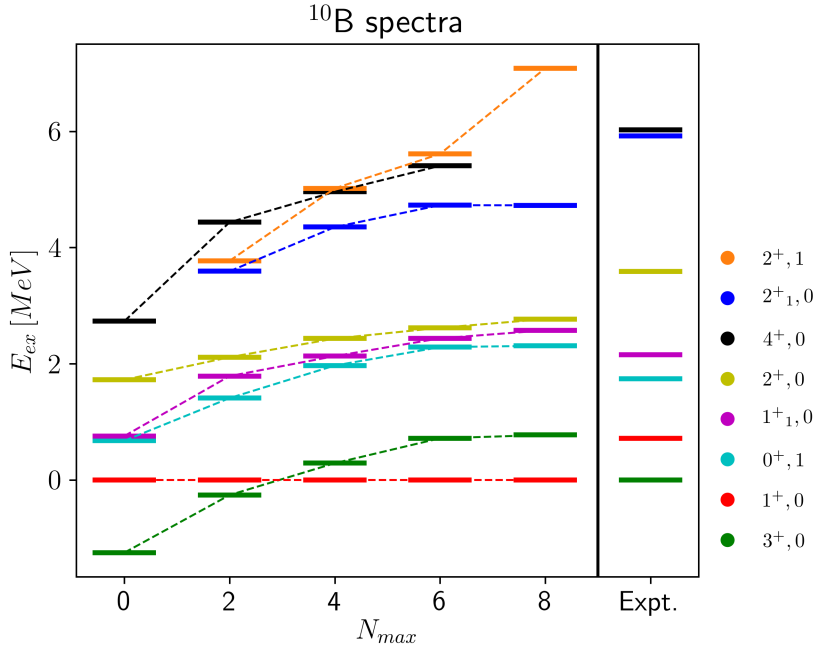

Figure 6: Excitation spectra for ^{10}B using the $NN - N^4LO(500)$ interaction. A $\lambda_{SRG} = 1.8$ fm^{-1} is used with an $\hbar\Omega = 20$ MeV. Legend labels are J_n^{Parity}, $\tau_{isospin}$. Experimental results are shown in the right-most column.

Clearly, the $N_{\max} = 8$ results shown in Fig. 6 do not align well with experimentally determined results. As seen from ground state convergence results, it seems that lowest level excitations can be approximately reproduced by $NN - N^4LO(500)$ potentials, but any higher level excitations include complicated dynamics which cannot be well reproduced by merely two-body interactions. If we consider a lighter nucleus, such as ^{6}He, we find surprising agreement with experimental results, even though ^{6}He has an exotic structure. This may be due to the fact that the central alpha cluster and orbiting two-nucleon cluster can both be well described by a two-body interaction given the low number of interacting nucleons and their separation.

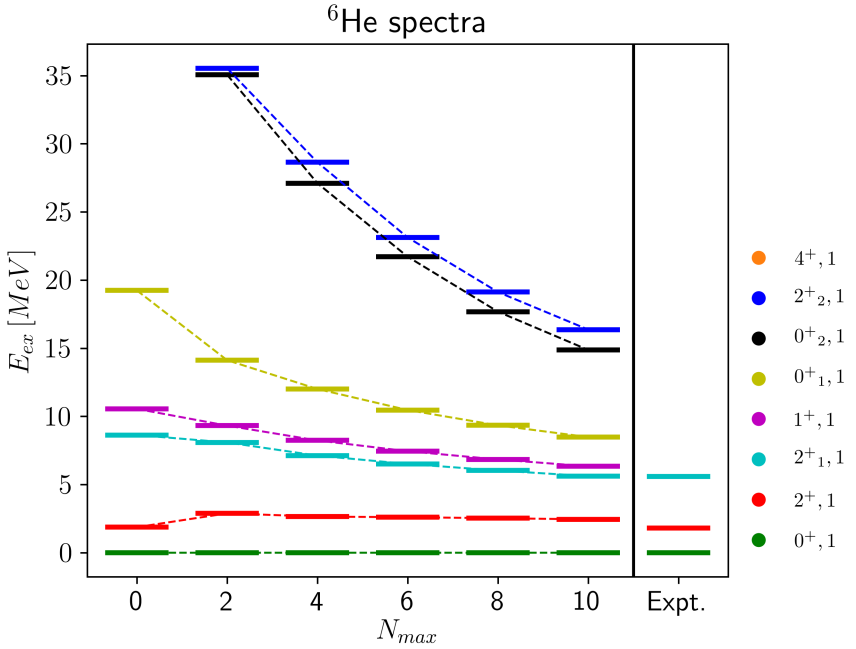

Figure 7: Excitation spectra for ^{6}He using the $NN - N^4LO(500)$ interaction. A $\lambda_{SRG} = 1.8$ fm^{-1} is used with an $\hbar\Omega = 20$ MeV. Legend labels are J_n^{Parity}, $\tau_{isospin}$. Experimental results are shown in the right-most column.

This is further shown by considering the spectra of ^{6}Li, which has the same number of nucleons but is a well bound nucleus with no central cluster. Results for the excitation spectra can be seen in Fig. 8, where we find that

the experimental values are again misaligned with theoretical predictions. In certain instances, we even find that some states converge faster than others, making the overall predicted structure incorrect.

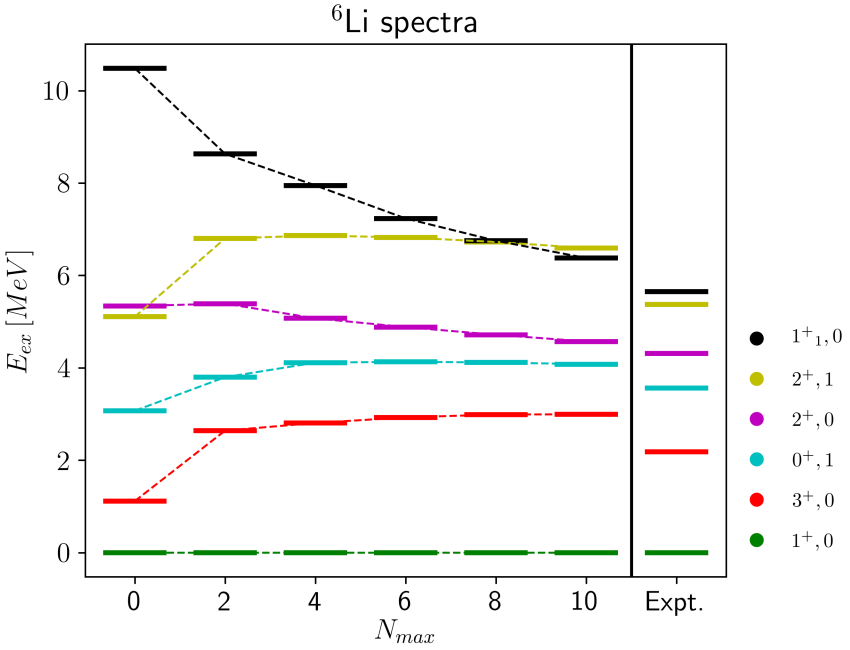

Figure 8: Excitation spectra for ^{6}Li using the $NN - N^4LO(500)$ interaction. A $\lambda_{SRG} = 1.8$ fm^{-1} is used with an $\hbar\Omega = 20$ MeV. Legend labels are J_n^{Parity}, $\tau_{isospin}$. Experimental results are shown in the right-most column.

We do not require further analysis to show that the $NN - N^4LO(500)$ interaction alone is incapable of describing nuclear excitation spectra. Even though the interaction worked surprisingly well in the case of exotic ^{6}He, we mostly obtain predictions inconsistent with experimental results.

2.2 Three-body Interactions

2.2.1 Ground state energy convergence

The three-body potentials for which results are presented have been computed to third order of the chiral EFT expansion for the three-nucleon interaction. As the maximum order achieved is third, this shall be labeled as next-to-next-to-leading order (N^2LO). Low energy constants (LECs), labeled c_i, were chosen as in Ref. [7], while the LECs c_D and c_E have been determined in $A = 3, 4$ systems. This 3N component of the potentials serves as a powerful refinement for our *ab initio* nuclear structure calculations. Further, we shall denote this contribution to the nuclear potential as $3N - N^2LOlnl$, where 3N refers to the three-body component, N^2LO refers to the chiral EFT truncation, and lnl refers to the local and nonlocal regularization being applied, with the respective cutoffs of 650 MeV and 500 MeV [12]. The total form of the potential we are using is then written as $NN - N^4LO(500) + 3N - N^2LOlnl$. We also introduce the $NN - N^4LO(500) + 3N - N^2LOE7lnl$ interaction, which differs by having the c_E coefficient determined from fitting of spectroscopic factors from varying beta decay overlap functions [18, 19, 20].

We have included the $NN - N^4LO(500) + 3N - N^2LOlnl$ interaction in the calculation of nonlocal translationally invariant one-body nuclear densities and intermediate-energy optical potentials of $s-$ and $p-$shell nuclei [21]. Thus, we have established that the unitarity of the SRG evolution of the 3N component is under control for the range of λ_{SRG} values and $\hbar\Omega$ parameter choice shown in section 2.1. It should be noted that the $N_{\max} = 8$ calculations for ^{12}C and ^{16}O were obtained using importance-truncated

NCSM basis as described in Ref. [22, 23].

In Fig. 9, we show results for the convergence of the ground state energies of ^{4}He using the new $NN - N^4LO(500) + 3N - N^2LOlnl$ interaction. We can again see the benefit of using SRG evolved interactions with the 3N terms. It is important to notice the significant change to the ground state energy achieved by the three-body potentials. We see large improvements all around, with the $N_{\max}$ converged results yielding a ground state energy of -28.16 MeV, compared to -26.65 MeV for the $NN - N^4LO(500)$ interaction.

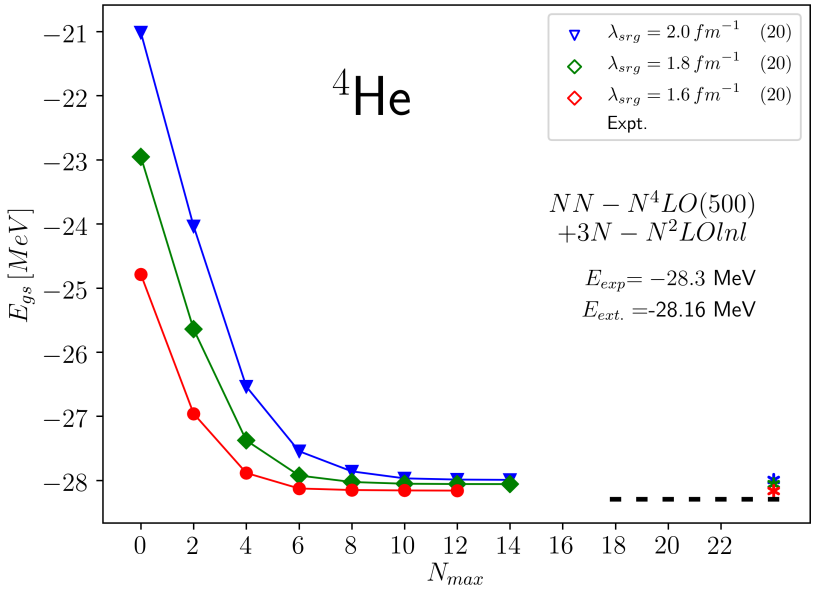

Figure 9: Convergence of ground state energy for ^{4}He using the $NN - N^4LO(500) + 3N - N^2LOlnl$ interaction. SRG parameters of 2.0, 1.8, and 1.6 fm^{-1} are shown using an $\hbar\Omega = 20$ MeV. Extrapolated energies are shown with starred markers. Experimental data is shown with black lines.

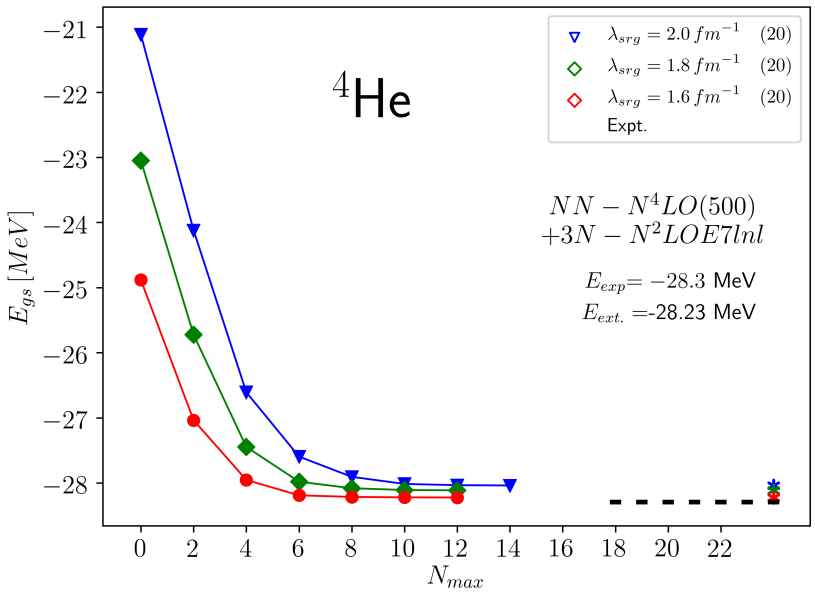

Figure 10: Convergence of ground state energy for ^{4}He using the $NN - N^4LO(500) + 3N - N^2LOE7lnl$ interaction. SRG parameters of 2.0, 1.8, and 1.6 fm^{-1} are shown using an $\hbar\Omega = 20$ MeV. Extrapolated energies are shown with starred markers. Experimental data is shown with black lines.

Notice the slight differences between Fig. 10 and Fig. 9. It appears that the method of fitting spectroscopic factors further refines our predictive powers in calculations of the ground state energy. We see improvements to the extrapolated values for the $NN - N^4LO(500) + 3N - N^2LOE7lnl$ interaction with results of −28.23 MeV, as opposed to −28.16 MeV for the $NN - N^4LO(500) + 3N - N^2LOlnl$ interaction.

Similar results can be shown in comparisons for ^{6}He. In Fig. 11, we see extremely larger improvements in the predictions for the ground state energy of the exotic nucleus ^{6}He. When using the $NN - N^4LO(500)$ interaction, our extrapolation produced −26.4 MeV as the predicted ground state of ^{6}He. Implementing our new three-body interactions and performing the same process yields a much more reasonable result of −28.69 MeV. This 3N

interaction is able to close the gap between theory and experiment by several MeV. We still find, however, that the agreement is not perfect. It is thus important to construct more terms in the chiral expansion and attempt to increase binding in the nucleus, further refining our results. If this is ineffective, we may be required to move to four-body interactions, which can increase the complexity of the calculation by several orders of magnitude.

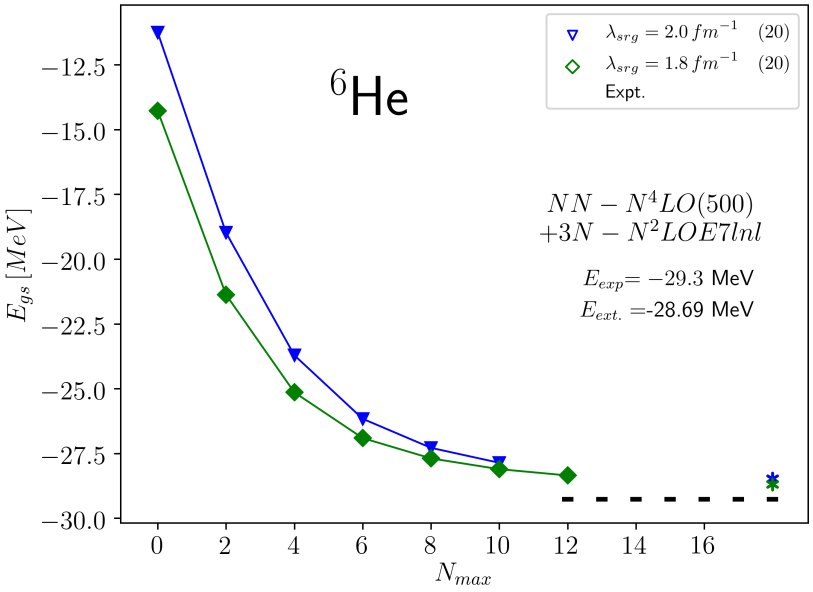

Figure 11: Convergence of ground state energy for ^{4}He using the $NN - N^4LO(500) + 3N - N^2LOE7lnl$ interaction. SRG parameters of 2.0, 1.8, and 1.6 fm^{-1} are shown using an $\hbar\Omega = 20$ MeV. Extrapolated energies are shown with starred markers. Experimental data is shown with black lines.

We now consider ^{6}Li, for which results are shown with both types of three-body interactions in Fig. 12 and Fig. 13. Here, we see rather different convergence patterns for the results, even though the ground state energy predictions are rather similar. The most important difference between the two interactions is that the $NN - N^4LO(500) + 3N - N^2LOE7lnl$ interaction very closely reproduces the ground state energy of ^{6}Li, only under binding the experimental result by 0.2 MeV.

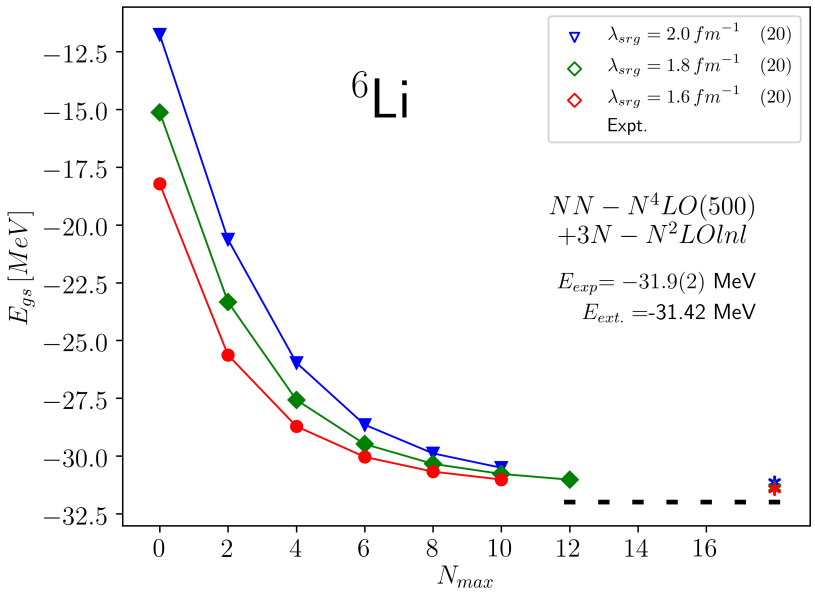

Figure 12: Convergence of ground state energy for ^{6}Li using the $NN - N^4LO(500) + 3N - N^2LOlnl$ interaction. SRG parameters of 2.0, 1.8, and 1.6 fm^{-1} are shown using an $\hbar\Omega = 20$ MeV. Extrapolated energies are shown with starred markers. Experimental data is shown with black lines.

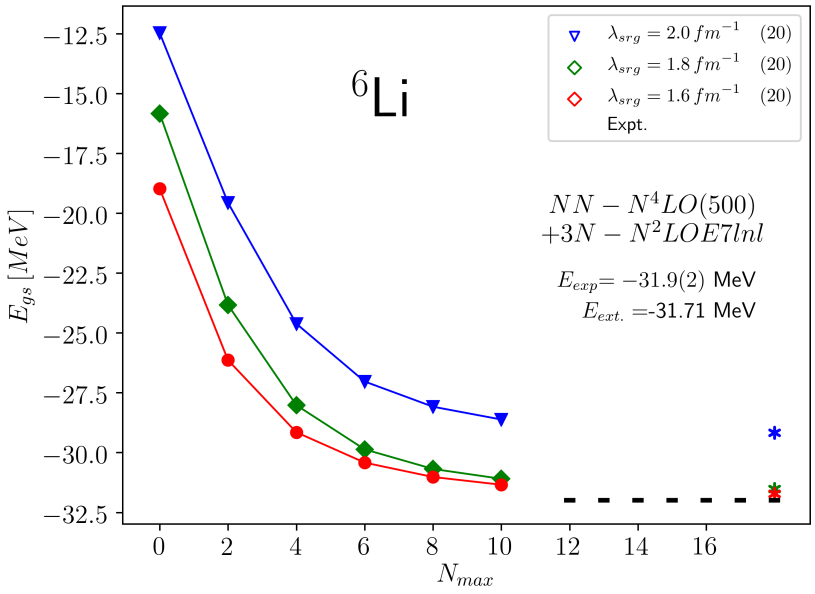

Figure 13: Convergence of ground state energy for ^{6}Li using the $NN - N^4LO(500) + 3N - N^2LOE7lnl$ interaction. SRG parameters of 2.0, 1.8, and 1.6 fm^{-1} are shown using an $\hbar\Omega = 20$ MeV. Extrapolated energies are shown with starred markers. Experimental data is shown with black lines.

Another noteworthy point is the visible stability of the $NN - N^4LO(500) + 3N - N^2LOlnl$ interaction. At $N_{\max} = 10$, we see very small dependencies on the λ_{SRG} wave flow parameter. All of the extrapolated results lie closely above one another, as expected. However, when looking at the $NN - N^4LO(500) + 3N - N^2LOE7lnl$ interaction, we see drastic instabilities in the predicted results with $\lambda_{SRG} \geq 1.8$ fm^{-1}. The sensitivity to the wave flow parameter means that we must be more careful with our parameter choices when dealing with this type of potential.

Comparing ^{12}C results between the two-body and two- plus three-body interactions, we see massive improvements in our theoretical predictions. Using the $NN - N^4LO(500) + 3N - N^2LOE7lnl$ interaction, we yield an extrapolated ground state energy of -91.11 MeV, as opposed to the prediction of -84.24 MeV generated from the two-body potentials.

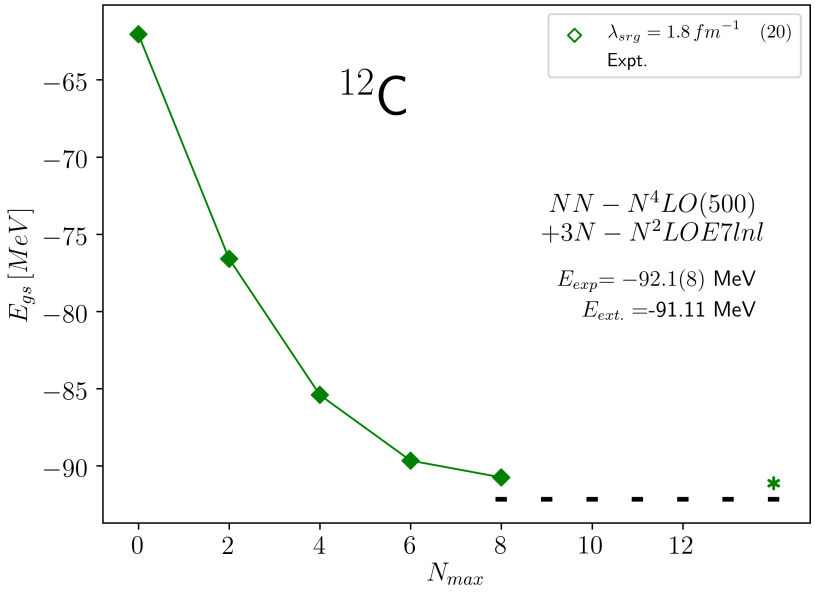

Figure 14: Convergence of ground state energy for ^{12}C using the $NN - N^4LO(500) + 3N - N^2LOE7lnl$ interaction. An SRG parameter of 1.8 fm^{-1} is shown using an $\hbar\Omega = 20$ MeV. Extrapolated energies are shown with starred markers. Experimental data is shown with black lines.

The results shown above alone provide strong evidence for the necessity of including three-body interactions in our calculations. For completion, we include the results of ^{16}O and ^{3}H in Fig. 15 and Fig. 16, respectively. In oxygen, we still see strong convergence issues, with certain points most likely belonging to failed calculations. Considering we are using the more stable $NN - N^4LO(500) + 3N - N^2LOlnl$ interaction, it is unfortunate that we still obtain very strong dependence on the λ_{SRG} parameter.

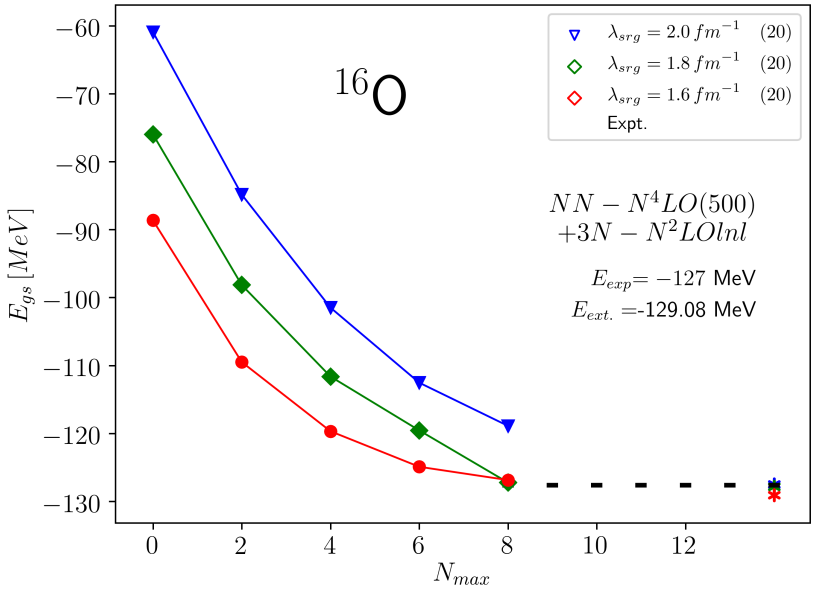

Figure 15: Convergence of ground state energy for ^{16}O using the $NN - N^4LO(500) + 3N - N^2LOlnl$ interaction. SRG parameters of 2.0, 1.8, and 1.6 fm^{-1} are shown using an $\hbar\Omega = 20$ MeV. Extrapolated energies are shown with starred markers. Experimental data is shown with black lines.

We include the results of ^{3}H in Fig. 16 to show the accuracy and predictive ability of NN plus 3N potentials. The λ_{SRG} dependence vanishes as expected, and we are able to exactly reproduce the experimental measurement of the ground state of ^{3}H, which should come as no surprise given this nucleus is a three-body system.

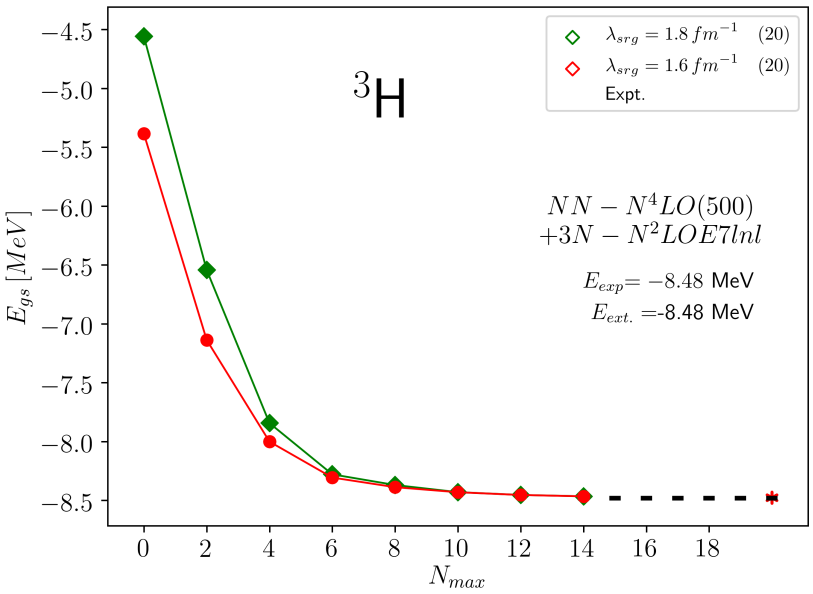

Figure 16: Convergence of ground state energy for ^{3}H using the $NN - N^4LO(500) + 3N - N^2LOE7lnl$ interaction. SRG parameters of 1.8 and 1.6 fm^{-1} are shown using an $\hbar\Omega = 20$ MeV. Extrapolated energies are shown with starred markers. Experimental data is shown with black lines.

It is clear from the analysis that inclusion of three-body interactions is necessary if we are to produce more accurate predictions of nuclear observables. Further work must be done in order to improve our three-body additions to the shell model, and to hopefully reduce the requirement to move to four-body terms.

2.2.2 Excitation spectra

We will now return to the excitation spectra of nuclei using the
$NN - N^4LO(500) + 3N - N^2LOlnl$ and
$NN - N^4LO(500) + 3N - N^2LOE7lnl$ potentials.

Draw your attention to Fig. 17 and Fig. 18, which each show one version of

the 3N potential. The first noteworthy feature of these figures is that the inclusion of the three-body interactions has produced results which correctly predict the ground state of ^{10}B, which the NN interaction was incapable of doing. Comparing the two figures, one ascertains several non-trivial differences between the results of the two interactions. For example, when using the $NN - N^4LO(500) + 3N - N^2LOlnl$ interaction, we notice that the $(1_1^+, 0)$ (first excited $(1^+, 0)$ state) is weakly bound and pushed well below the experimental result, swapping places with the $(0^+, 1)$ state. In fact, we notice that in many high-lying excitations, the theoretical predictions fall below their experimental counterparts, implying that this interaction is binding the nucleus too weakly. Looking at results from the $NN - N^4LO(500) + 3N - N^2LOE7lnl$ interaction, we see that the swapping of the $(0^+, 1)$ and the $(1_1^+, 0)$ is corrected. However, we pay the price for other states. We see that many gaps between excited states are reduced, pushing states J_n^{Parity}, τ closer to its next excited state, J_{n+1}^{Parity}, τ. This interaction interestingly causes many of the low-lying excitations to now be over bound, pushing the energies above experimental values, while high-lying excitations are pushed closer to their corresponding experimental results. These results indicate a strong dependency on the c_E coefficient in the chiral expansion, which is responsible for a variety of different nuclear effects. If these results are to be well understood, a heavier investigation of the coefficient determination must be undertaken. It should be noted that we do not expect good convergence to experimental results in high-lying states such as the $(2^+, 1)$, the $(3_1^+, 0)$, and the $(2_1^+, 0)$ as these excitations are too high to currently be handled well by the NCSM.

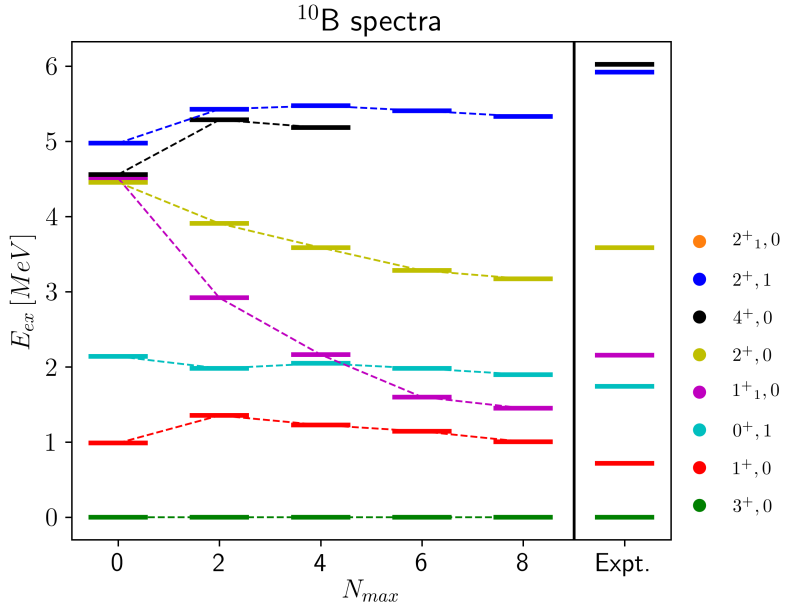

Figure 17: Excitation spectra for ^{10}B using the $NN - N^4LO(500) + 3N - N^2LOlnl$ interaction. A $\lambda_{SRG} = 1.8$ fm^{-1} is used with an $\hbar\Omega = 20$ MeV. Legend labels are J_n^{Parity}, $\tau_{isospin}$. Experimental results are shown in the right-most column.

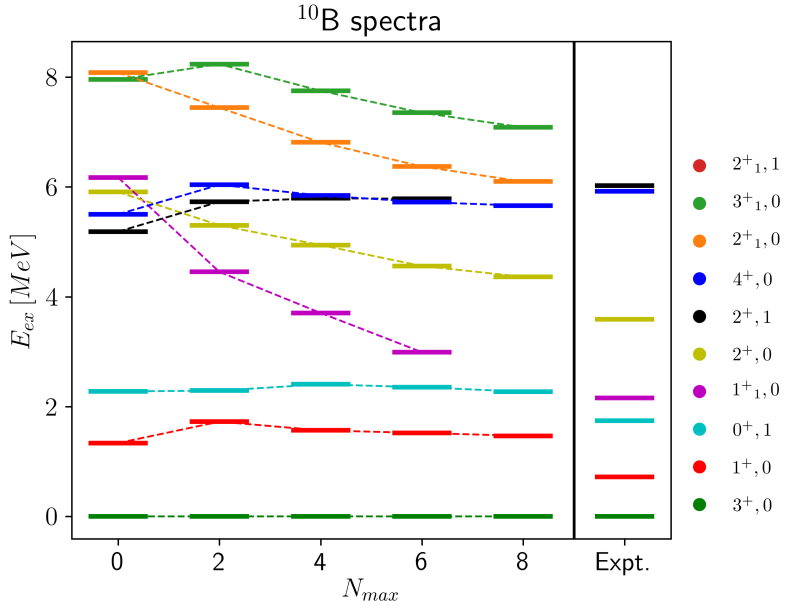

Figure 18: Excitation spectra for ^{10}B using the $NN - N^4LO(500) + 3N - N^2LOE7lnl$ interaction. A $\lambda_{SRG} = 1.8$ fm^{-1} is used with an $\hbar\Omega = 20$ MeV. Legend labels are J_n^{Parity}, $\tau_{isospin}$. Experimental results are shown in the right-most column.

If we now look at Fig. 19, which shows the spectra of ^{6}He, we notice that there are not many significant changes between the two- and two- plus three-body results. It appears that majority of the physics pertaining to excitations of ^{6}He can be captured by solely two-body interactions. This is most likely due to the alpha core ($A = 4$) plus two-neutron orbiting pair ($A = 2$) being loosely bound to one another and having majority of the energy coming components interacting primarily in their respective groups.

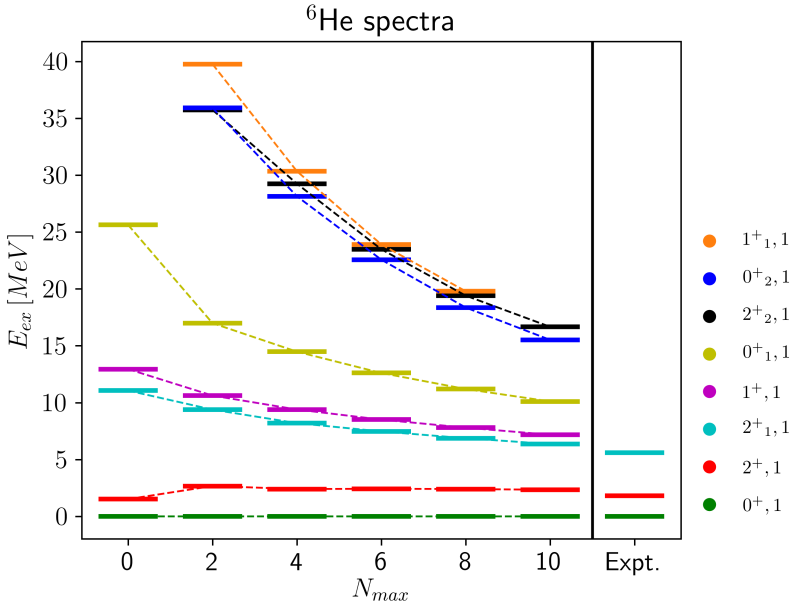

Figure 19: Excitation spectra for ^{6}He using the $NN - N^4LO(500) + 3N - N^2LOE7lnl$ interaction. A $\lambda_{SRG} = 2.0$ fm^{-1} is used with an $\hbar\Omega = 20$ MeV. Legend labels are J_n^{Parity} , $\tau_{isospin}$. Experimental results are shown in the right-most column.

Refer now to Fig. 20 and Fig. 21, which are plots of the excitation energies of ^{6}Li using the $3N - N^2LOlnl$ and $3N - N^2LOE7lnl$ three-body potentials, respectively.

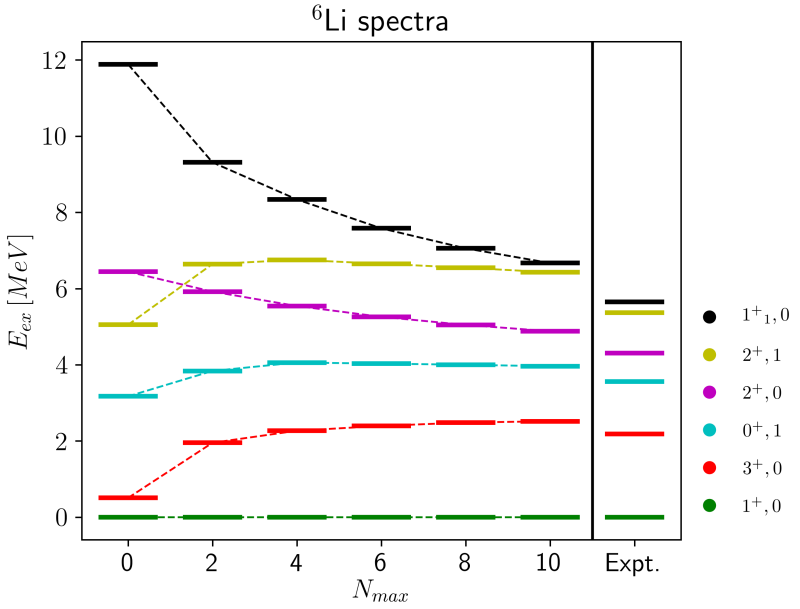

Figure 20: Excitation spectra for ^{6}Li using the $NN - N^4LO(500) + 3N - N^2LOlnl$ interaction. A $\lambda_{SRG} = 1.6$ fm^{-1} is used with an $\hbar\Omega = 20$ MeV. Legend labels are J_n^{Parity}, $\tau_{isospin}$. Experimental results are shown in the right-most column.

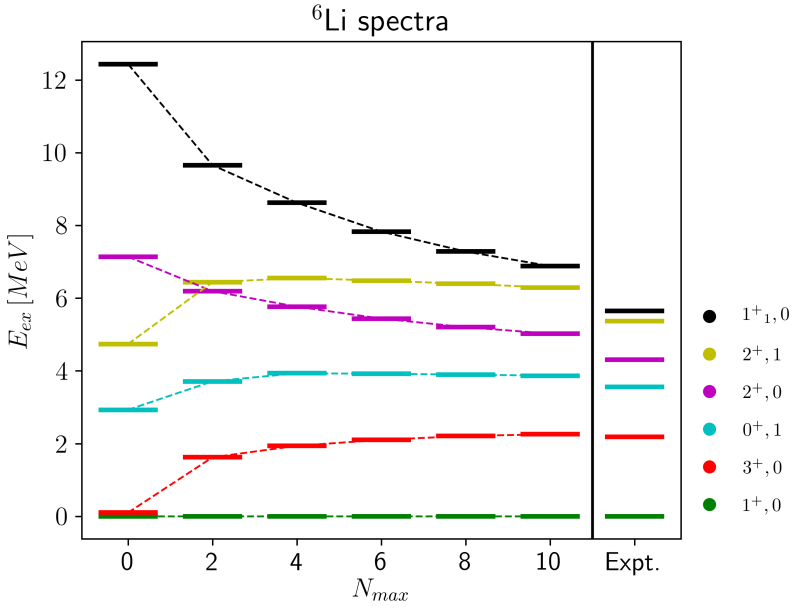

Figure 21: Excitation spectra for ^{6}Li using the $NN - N^4LO(500) + 3N - N^2LOE7lnl$ interaction. A $\lambda_{SRG} = 1.6$ fm^{-1} is used with an $\hbar\Omega = 20$ MeV. Legend labels are J_n^{Parity}, $\tau_{isospin}$. Experimental results are shown in the right-most column.

Implementing the three-body potentials has certainly improved the predictions for spectra of ^{6}Li. For both 3N interactions, we see all around improvements in the NCSM's ability to produce more accurate excitations energies. Noticeably, gaps between the $(3^+, 0)$, the $(0^+, 1)$, and the $(2^+, 0)$ states are all widened. This implies that couplings between different states have been weakened by the inclusion of a three-body force. We notice that gaps between $(2^+, 1)$ and the $(1_1^+, 0)$ have also been widened, and these new three-nucleon interactions are capable of preventing these states from crossing one another. This effect of widening is important, more so in the c_E adjusted 3N interaction, as it pushes all low-lying spectra much closer to experiment. Noticeably, we have that the $(2^+, 0)$ and the $(1_1^+, 0)$ have been pushed too far from experiment relative to the predictions of $3N - N^2LOlnl$ three-body potentials.

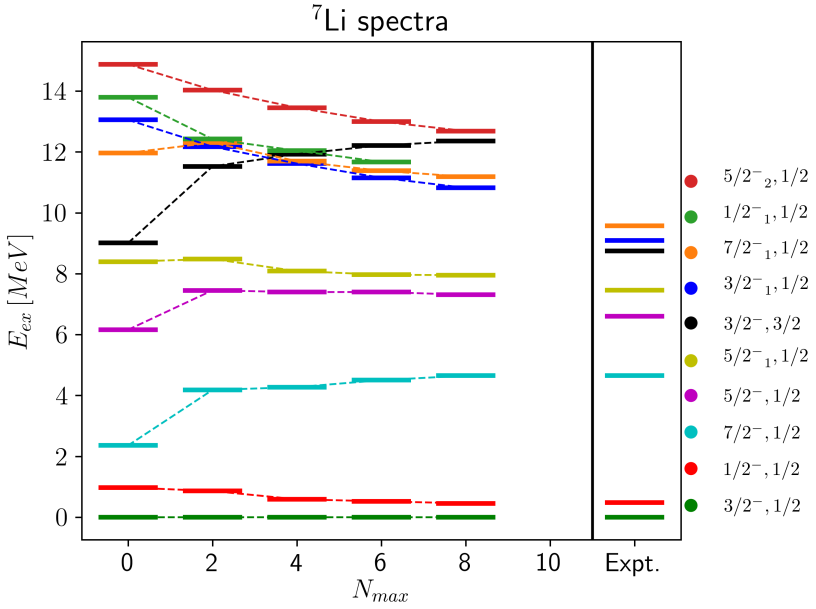

Figure 22: Excitation spectra for ^{7}Li using the $NN - N^4LO(500) + 3N - N^2LOE7lnl$ interaction. A $\lambda_{SRG} = 2.0$ fm^{-1} is used with an $\hbar\Omega = 20$ MeV. Legend labels are J_n^{Parity}, $\tau_{isospin}$. Experimental results are shown in the right-most column.

We can also use the $NN - N^4LO(500) + 3N - N^2LOE7lnl$ interaction to look at the spectra of ^{7}Li and ^{8}Li. In Fig. 22, we see that the first five states of ^{7}Li are reproduced very well in our model, with certain states being only slightly over bound. The same is true for ^{8}Li, shown in Fig. 23. The experimental values line up very well with the theoretical predictions at $N_{\max} = 8$.

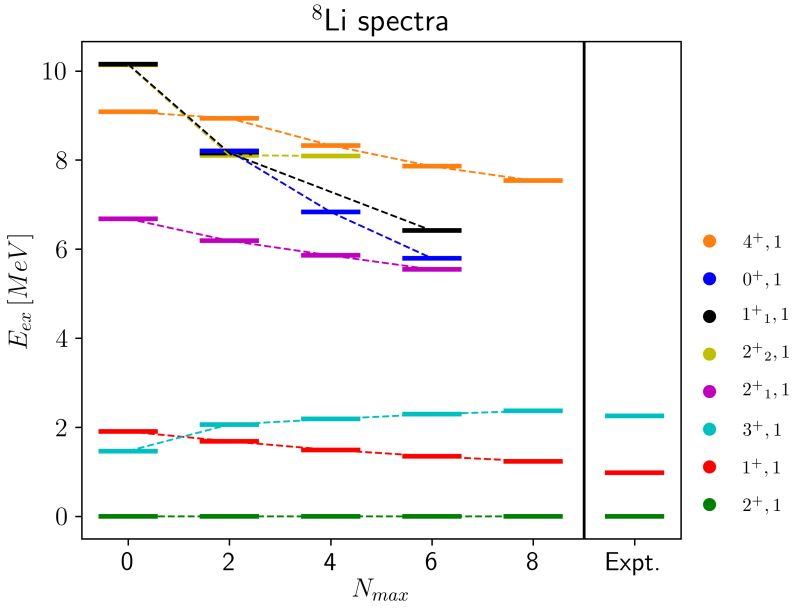

Figure 23: Excitation spectra for ^{8}Li using the $NN - N^4LO(500) + 3N - N^2LOE7lnl$ interaction. A $\lambda_{SRG} = 1.8$ fm^{-1} is used with an $\hbar\Omega = 20$ MeV. Legend labels are J_n^{Parity} , $\tau_{isospin}$. Experimental results are shown in the right-most column.

The results obtained for all systems with the three-body potentials are promising given their relative stability in the observed systems. Evidently, these new interactions are stable under the conditions in which we apply them and they provide strong improvements in our results, so we expect that the use of the three-body terms shall become a necessary implementation in future calculations.

3.0 Conclusions

The purpose of this work was to analyze the inclusion of two- and three-body chiral EFT potentials in the NCSM framework for achieving more physically consistent calculations. Comparing the two-body interactions to the two- plus three-body interactions, one finds sizable improvements stemming from the inclusion of 3N terms in the chiral expansion. This is done successfully with minor impacts on computation time, ensuring that the inclusion of 3N terms should be sufficiently beneficial. What is found in the analysis is that the three-body components of the interactions provide very large corrections to the two-body results, often providing refined results in our predictions for light nuclei.

In terms of ground state energy convergence results, we saw, for most nuclei, strong convergence trends and improved extrapolated results when employing the additional three-body interactions. This was true also in the case of studying exotic nuclei, such as ^{6}He, which in the past have proven difficult to treat for the NCSM. In general, we found the $NN - N^4LO(500)$ $+3N - N^2LOlnl$ interaction to be more stable and produce improved results, whereas the $NN - N^4LO(500) + 3N - N^2LOE7lnl$ interaction was less stable but produced more refined results using a $\lambda_{SRG} = 1.8$ fm^{-1}.

When studying the excitation spectra of nuclei, we quickly determined that the two-body interaction alone is incapable of describing most systems within any reasonable uncertainty. This fact was remedied by inclusion of the three-body terms, which then significantly improved spectra predictions in several nuclei. Nevertheless, we still find that 3N terms are not enough to consistently calculate the excitation spectra of nuclei, with many states

having a strong dependence of the c_E coefficient in our chiral expansion.

The motion to include higher-body terms at larger $N_{\max}$ is continuing in this manner, with many efforts to reduce basis sizes and provide more advanced extrapolation for future results. Clearly, the three-body terms are a significant contributor to the wave function of the nucleus, and should certainly be included with the largest possible truncation to obtain the most physically accurate and converged theoretical prediction.

4.0 Recommendations

It is recommended that additional improvements in convergence be achieved before continuing to higher-body terms, or before pushing three-body terms to a higher order of the chiral expansion. For many nuclei, we teeter on the edge of unreasonable computation time, and pushing our theoretical framework further will not yield and useful computational results without first improving the convergence rate and handling of the implemented framework in various codes.

Further investigation of the c_E coefficient and the specific physics it encapsulates is required if we are to better determine it for potentials which can treat a wider range of nuclei. A new attempt in process is to fit the spectroscopic factors of triton beta decay, which produces highly accurate experimental data for fitting this c_E term. This may lead us to improve our three-body potentials and produce an additional step of consistency in our calculations.

References

[1] R. Machleidt and D. R. Entem, "Chiral effective field theory and nuclear forces," *Physics Reports*, vol. 503, no. 1, pp. 1–75, 2011.

[2] B. R. Barrett, P. Navrátil, and J. P. Vary, "Ab initio no core shell model," *Progress in Particle and Nuclear Physics*, vol. 69, pp. 131–181, 2013.

[3] F. Wegner, "Flow-equations for hamiltonians," *Annalen der physik*, vol. 506, no. 2, pp. 77–91, 1994.

[4] S. Bogner, R. Furnstahl, and R. Perry, "Similarity renormalization group for nucleon-nucleon interactions," *Physical Review C*, vol. 75, no. 6, p. 061001, 2007.

[5] R. Roth, S. Reinhardt, and H. Hergert, "Unitary correlation operator method and similarity renormalization group: Connections and differences," *Physical Review C*, vol. 77, no. 6, p. 064003, 2008.

[6] S. Bogner, R. Furnstahl, and A. Schwenk, "From low-momentum interactions to nuclear structure," *Progress in Particle and Nuclear Physics*, vol. 65, no. 1, pp. 94–147, 2010.

[7] D. Entem, R. Machleidt, and Y. Nosyk, "High-quality two-nucleon potentials up to fifth order of the chiral expansion," *Physical Review C*, vol. 96, no. 2, p. 024004, 2017.

[8] B. A. Lippmann and J. Schwinger, "Variational principles for scattering processes. i," *Physical Review*, vol. 79, no. 3, p. 469, 1950.

[9] C. Joachain, *Quantum collision theory*. North-Holland, 1975.

[10] W. Glöckle, *The quantum mechanical few-body problem*. Texts and monographs in physics, Springer-Verlag, 1983.

[11] R. Newton, *Scattering Theory of Waves and Particles*. Theoretical and Mathematical Physics, Springer Berlin Heidelberg, 2013.

[12] P. Navratil, "Local three-nucleon interaction from chiral effective field theory," *Few-Body Systems*, vol. 41, no. 3, pp. 117–140, 2007.

[13] TUNL, *Energy Level Diagram, ^{10}B (2004)*, 2004.

[14] TUNL, *Energy Level Diagram, ^{6}He (2002)*, 2002.

[15] TUNL, *Energy Level Diagram, ^{6}Li (2002)*, 2002.

[16] TUNL, *Energy Level Diagram, ^{7}Li (2002)*, 2002.

[17] TUNL, *Energy Level Diagram, ^{8}Li (2004)*, 2004.

[18] N. Timofeyuk, "Overlap functions, spectroscopic factors, and asymptotic normalization coefficients generated by a shell-model source term," *Physical Review C*, vol. 81, no. 6, p. 064306, 2010.

[19] M. Stoitsov, S. Dimitrova, and A. Antonov, "Restoration of overlap functions and spectroscopic factors in nuclei," *Physical Review C*, vol. 53, no. 3, p. 1254, 1996.

[20] C. Clement, "Theory of overlap functions:(i). single particle sum rules and centre-of-mass corrections," *Nuclear Physics A*, vol. 213, no. 3, pp. 469–492, 1973.

[21] M. Gennari, M. Vorabbi, A. Calci, and P. Navratil, "Microscopic optical potentials derived from ab initio translationally invariant nonlocal one-body densities," *arXiv preprint arXiv:1712.02879*, 2017.

[22] R. Roth and P. Navrátil, "Ab initio study of ca 40 with an importance-truncated no-core shell model," *Physical review letters*, vol. 99, no. 9, p. 092501, 2007.

[23] R. Roth, "Importance truncation for large-scale configuration interaction approaches," *Physical Review C*, vol. 79, no. 6, p. 064324, 2009.